Original Article

IRF7 and *IFIT2* in mediating different hemorrhage outcomes for non-small cell lung cancer after bevacizumab treatment

Liuying Huang[1,2#], Yuan Yin[1#], Danqi Qian[2#], Yulin Cao[1], Duo Wang[1,2], Xiaohan Wu[1], Liang Ming[1], Zhaohui Huang[1], Leyuan Zhou[2,3,4]

[1]Wuxi Cancer Institute, Affiliated Hospital of Jiangnan University, Wuxi, China; [2]Department of Radiation Oncology, Affiliated Hospital of Jiangnan University, Wuxi, China; [3]Department of Radiation Oncology, Dushu Lake Hospital Affiliated to Soochow University, Suzhou, China; [4]State Key Laboratory of Radiation Medicine and Protection, Soochow University, Suzhou, China

Contributions: (I) Conception and design: L Zhou, Y Yin, L Huang; (II) Administrative support: L Zhou, Y Yin, Z Huang; (III) Provision of study materials or patients: D Qian, D Wang; (IV) Collection and assembly of data: L Huang, D Qian, X Wu; (V) Data analysis and interpretation: Y Yin, L Huang, Y Cao, L Ming; (VI) Manuscript writing: All authors; (VII) Final approval of manuscript: All authors.

[#]These authors contributed equally to this work.

Correspondence to: Zhaohui Huang. Wuxi Cancer Institute, Affiliated Hospital of Jiangnan University, Wuxi 214062, China.
Email: zhaohuihuang@jiangnan.edu.cn; Leyuan Zhou. Department of Radiation Oncology, Affiliated Hospital of Jiangnan University, Wuxi, China; Department of Radiation Oncology, Dushu Lake Hospital Affiliated to Soochow University, Suzhou 215000, China; State Key Laboratory of Radiation Medicine and Protection, Soochow University, Suzhou, China. Email: zhouleyuan99@126.com.

Background: Lung cancer has some of the highest morbidity and mortality worldwide among cancers, with non-small cell lung cancer (NSCLC) accounting for 85% of lung cancer diagnoses. Severe pulmonary hemorrhage (PH) is a serious potential adverse event in the treatment of lung cancer with bevacizumab. Significant clinical differences have been observed between patients with lung adenocarcinoma (LUAD) and those with lung squamous cell carcinoma (LUSC) after bevacizumab treatment; however, the underlying causes is unclear and requires further study.

Methods: First, tumor tissues from LUAD and LUSC patients were stained with antibodies targeting CD31 and CD34 to assess the difference in microvessel density (MVD). Tube formation assays were performed using HMEC-1 cells cocultured with lung cancer cells. Single-cell sequencing data obtained from lung cancer tissues were then downloaded and analyzed to identify differentially expressed genes related to angiogenesis in LUAD and LUSC tumors. Real-time polymerase chain reaction, immunofluorescence analysis, small interfering RNA analysis, and enzyme-linked immunosorbent assay were performed to clarify the underlying causes.

Results: The MVD of LUAD tissues was higher than that of LUSC tissues. Additionally, endothelial cells cocultured with LUAD cells had a higher MVD than did those cocultured with LUSC cells. Although bevacizumab mainly targets vascular endothelial growth factor (*VEGF*), the expression of *VEGF* in LUSC and LUAD cells was not significantly different (P>0.05). Further experiments showed that interferon regulatory factor 7 *(IRF7*) and interferoninduced protein with tetratricopeptide repeats 2 (*IFIT2*) were differentially expressed between LUSC and LUAD tumors. Higher *IRF7* levels and lower *IFIT2* levels in LUAD tumors were associated with higher MVD in LUAD tissues, which may be responsible for the different hemorrhage outcomes after bevacizumab treatment.

Conclusions: Our data indicated that *IRF7* and *IFIT2* may account for the differential hemorrhage outcomes in patients with NSCLC after bevacizumab treatment, revealing a new mechanism underlying bevacizumab-induced pulmonary hemoptysis.

Keywords: Non-small cell lung cancer (NSCLC); angiogenesis; bevacizumab; pulmonary hemoptysis

Submitted Feb 15, 2023. Accepted for publication Apr 20, 2023. Published online Apr 26, 2023.
doi: 10.21037/jtd-23-389
View this article at: https://dx.doi.org/10.21037/jtd-23-389

Introduction

Lung cancer is among the cancers with the highest morbidity and mortality in the world (1). There are approximately 2 million new lung cancer cases and 1.76 million lung cancer deaths per year. Lung cancers can be classified as non-small cell lung cancer (NSCLC; 85% of total diagnoses) and small cell lung cancer (SCLC; 15% of total diagnoses) (2). However, approximately 70% of patients with NSCLC are already in advanced disease stages at the time of their first diagnosis, and these patients have a poor 5-year survival, with only 10–20% surviving past this period (3).

Traditional radiation therapy and chemotherapy strategies are usually unable to meet therapeutic expectations (4). In recent years, molecular targeted therapy and immunotherapy have substantially improved patient survival (5-9). Bevacizumab, a recombinant humanized anti-vascular endothelial growth factor (*VEGF*) monoclonal antibody, is one of the most important targeted drugs for a range of advanced cancers with poor prognosis, including NSCLC (10,11). However, in a phase II clinical study, Margolin *et al.* found that bevacizumab treatment in patients with advanced NSCLC caused a substantial adverse reaction in the form of bleeding, which was more common in patients with lung squamous cell carcinoma (LUSC) than in those with lung adenocarcinoma (LUAD) (12); furthermore, based on the pivotal E4599 study, bevacizumab has only been approved for patients with nonsquamous NSCLC (13).

Previous studies have suggested that hemoptysis caused by bevacizumab is related to anatomical characteristics. For example, LUSC is commonly thought to occur in the central airway, in which the pulmonary artery or branches are prone to rupture, with a high probability of substantial hemoptysis when tumors invade (14). However, in a prospective phase II trial involving patients with lung cancers at high risk of hemoptysis, Hellmann *et al.* evaluated the safety of adjuvant bevacizumab following neoadjuvant chemotherapy and complete surgical resection. They observed no instances of hemoptysis of any grade in patients with central tumors (15). Another study similarly found that no clinical or radiological features (including cavitation and central tumor location) could be used to reliably predict severe pulmonary hemorrhage in bevacizumab-treated patients (16). In a retrospective study involving 536 patients with pulmonary malignancy, Salajka *et al.* reported that the incidence of hemoptysis was similar between patients with central tumors and those with peripheral tumors. They also suggested that the occurrence of bleeding was related to the histological type of tumor and the tumor size (17). However, in a recent case-control study of risk factors for hemoptysis, multivariate analysis revealed that prior thoracic radiotherapy, the presence of tumor exposure in the central airway, and concomitant radiotherapy were risk factors for hemoptysis (18). This finding suggests that the substantial hemoptysis that occurs during bevacizumab treatment is not simply related to anatomical factors.

However, the reasons for the substantial clinical differences between patients with LUSC and those with LUAD receiving bevacizumab treatment are unclear. Additionally, there is no consensus on the correlation between microvessel density (MVD) and bleeding. Based on the evaluation of MVD, Iordache *et al.* found a clear correlation between angiogenic parameters and the risk of upper gastrointestinal bleeding in patients with gastric cancer (19). In contrast, some scholars believe that tumors with sufficient MVD do not exhibit activation of the hypoxia-induced signaling pathway and remain sensitive to chemotherapy and radiotherapy. The lack of involvement of such signaling pathways may lead to reduced tumor invasiveness. A low MVD is associated with higher tumor aggressiveness, resulting in higher levels of vascular infiltration and hemorrhage (20,21). In this study, we found that LUAD tumors had a higher MVD than did LUSC tumors. No significant difference in *VEGF* expression was observed between LUSC- and LUAD-associated endothelial cells. In addition, we found that there was strong heterogeneity between LUAD and LUSC endothelial cells. Moreover, *IFIT2* and *IRF7* were highly enriched in epithelial cells of NSCLC tumors, and

Highlight box

Key findings

- The microvessel density (MVD) of lung adenocarcinoma (LUAD) tissues was higher than that of lung squamous cell carcinoma (LUSC) tissues. Higher *IRF7* levels and lower *IFIT2* levels in LUAD tumors were associated with a higher MVD in LUAD tissues, which may be responsible for the different hemorrhage outcomes after bevacizumab treatment.

What is known and what is new?

- Significant clinical differences have been observed between LUAD and LUSC after bevacizumab treatment.
- *IRF7* and *IFIT2* may account for different hemorrhage outcomes in patients with non-small cell lung cancer.

What is the implication, and what should change now?

- The substantial hemoptysis caused by bevacizumab treatment can be prevented via targeting *IRF7* and *IFIT2* in patients with LUSC.

Table 1 Baseline characteristics of the study cohort

Variable	Total cohort (n=36)
Age (years)	62.9±7.9
Sex	
Male	27 (75.0)
Female	9 (25.0)
Pathology	
LUSC	18 (50.0)
LUAD	18 (50.0)
Differentiation	
Low	14 (38.9)
Moderate	18 (50.0)
Well	4 (11.1)
Stage	
I	8 (22.2)
II	14 (38.9)
III	12 (33.3)
IV	2 (5.6)
TNM	
T1	13 (36.1)
T2	13 (36.1)
T3	7 (19.5)
T4	3 (8.3)
N0	22 (61.1)
N1	5 (13.9)
N2	9 (25.0)
M0	34 (94.4)
M1	2 (5.6)

Data are expressed as number of patients (percentage) or mean ± SEM. LUAD, lung adenocarcinoma; LUSC, lung squamous cell carcinoma; SD, standard deviation; TNM, tumor-node-metastasis.

these two genes may underlie the differential hemorrhage outcomes in patients with NSCLC after bevacizumab treatment. These findings may provide new insights into the causes underlying bevacizumab-induced pulmonary hemoptysis. We present the following article in accordance with the MDAR and ARRIVE reporting checklists (available at https://jtd.amegroups.com/article/view/10.21037/jtd-23-389/rc).

Methods

Patients

Tumor tissues from 18 patients with LUSC and 18 patients with LUAD were obtained from the Affiliated Hospital of Jiangnan University (Wuxi, China). The pathophysiological information is displayed in *Table 1*. The study was approved by the Clinical Research Ethics Committees of Affiliated Hospital of Jiangnan University (No. LS2021019), and written informed consent was obtained from all patients. The study was conducted in accordance with the Declaration of Helsinki (as revised in 2013).

Cell culture

All cells were grown at 37 ℃ with 5% CO_2 in a humidified environment. HMEC-1 cells were grown in extracellular matrix (ECM). A549 cells and H358 cells were grown in high glucose Dulbecco's Modified Eagle Medium (DMEM) with 10% fetal bovine serum (FBS) and 1% penicillin/streptomycin. H2170 cells, H1703 cells, H1299 cells, and H226 cells were grown in RPMI 1640 with 10% FBS and 1% penicillin/streptomycin. Cells were confirmed to be mycoplasma free and were passaged no more than 18 to 25 times after thawing.

Immunohistochemistry

Tissue samples were fixed by immersion in 4% paraformaldehyde overnight at 4 ℃, embedded in regular paraffin wax, and cut into 4-μm sections. Sections were boiled in sodium citrate buffer (pH 6.0) for antigen retrieval, and endogenous peroxidase activity was blocked via incubation with 0.3% hydrogen peroxide. Sections were washed with 10% phosphate-buffered saline (PBS) and marked with a peroxidase-antiperoxidase (PAP) pen. After being blocked with 10% goat serum, the sections were incubated with primary antibodies against CD31 and CD34 for 12 h at 4 ℃. Finally, the samples were incubated with peroxidase-conjugated streptavidin. The images were developed by incubating the slides for several minutes with diaminobenzidine, and nuclei were counterstained with hematoxylin. The subsequent steps were performed using the EnVision FLEX High pH 9.0 Visualization System (Dako). All slides were independently evaluated by 2 pathologists. Microvessels clearly separated from adjacent brown-staining endothelial cells or endothelial cell clusters, tumor cells, and other connective-tissue elements

Table 2 Primer sequences

Gene	Forward primer (5'-3')	Reverse primer (5'-3')
VEGF	GAGGAGCAGTTACGGTCTGTG	TCCTTTCCTTAGCTGACACTTGT
VEGFA	GAGGGCAGAATCATCACGA	TGTGCTGTAGGAAGCTCATCTC
ISG15	CGCAGATCACCCAGAAGATCG	TTCGTCGCATTTGTCCACCA
LY6E	CAGCTCGCTGATGTGCTTCT	CAGACACAGTCACGCAGTAGT
IFI35	AACAAAAGGAGCACACGATCA	CTCCGTTCCTAGTCTTGCCAA
TXNIP	GGTCTTTAACGACCCTGAAAAGG	ACACGAGTAACTTCACACACCT
IFIT2	AAGCACCTCAAAGGGCAAAAC	TCGGCCCATGTGATAGTAGAC
IRF7	ATATCTCACGTGACCGAGGA	AGCTGATGGTGCTGGAAGTC
S100A8	ATGCCGTCTACAGGGATGAC	ACTGAGGACACTCGGTCTCTA
β-actin	AGTGTGACGTGGACATCCGCAAAG	ATCCACATCTGCTGGAAGGTGGAC

VEGF, vascular endothelial growth factor; *VEGFA*, vascular endothelial growth factor A; *ISG15*, interferon stimulated gene 15; *LY6E*, lymphocyte antigen 6; *IFI35*, interferon-induced protein 35; *TXNIP*, thioredoxin interacting protein; *IFIT2*, interferon-induced protein with tetratricopeptide repeats 2; *IRF7*, interferon regulatory factor 7; *S100A8*, S100 calcium binding protein A8.

were considered single, countable microvessels. We took photos and assessed the 3 areas with the highest MVD in each section under a 100× field of vision. All counts were performed simultaneously by 2 investigators (Y Yin and L Huang) using a light microscope, and both had to agree on what constituted a single microvessel before any vessel was included in the count.

Total RNA extraction and quantitative real-time polymerase chain reaction

Total RNA was extracted from cells using TRIzol reagent. Complement DNA (cDNA) was synthesized with a PrimeScript RT Reagent KIT (Vazyme China), quantitative real-time polymerase chain reaction (qRT-PCR) analyses were carried out to detect messenger RNA (mRNA) expression using SYBR Premix Ex Taq (Cwbio China), and β-actin was used as an internal control. Primer sequences are shown in *Table 2*.

Western blot analyses

Proteins were separated on a 10% sodium dodecyl-sulfate polyacrylamide gel electrophoresis (SDS-PAGE) gel and then transferred to polyvinylidene fluoride (PVDF) membranes. After being blocked with 5% nonfat milk, the membrane was incubated with mouse anti-*VEGF* and rabbit β-actin monoclonal antibodies. A peroxidase-conjugated anti-rabbit antibody was used as the secondary antibody, and the membranes were visualized with enhanced chemiluminescence.

Enzyme-linked immunosorbent assay

A549, H1299, H358, H2170, H226 and H1703 cells (1×10^5) were resuspended and plated in 24-well plates with 300 µL of complete medium, and the supernatant was collected after 3 days. Enzyme-linked immunosorbent assays (ELISA) were performed to evaluate the expression level of *VEGF* using ELISA kits (mlBio China) according to the manufacturer's instructions.

Immunofluorescence

Cell slides were placed in 6-well plates and seeded with the appropriate amount ofA549, H1299, H2170 and H226 cells overnight. After different treatments, the cells were washed 3 times with PBS, fixed with 4% paraformaldehyde for 20 minutes, and then blocked with 10% normal goat serum in PBS for 30 minutes at room temperature (RT). The next day, the cells were incubated with fluorescent secondary antibody for 1 hour at RT, stained with DAPI-containing mounting medium, and finally observed with a fluorescence microscope (#BX53F; Olympus).

Tube formation assay

Ice-cold phenol red Matrigel (300 µL) was added to a 24-well

plate using a chilled pipet tip and incubated for 3 hours at 37 ℃. HMEC-1 cells were cocultured with tumor cells for 72 hours. After coculture, the cells were washed twice with PBS and resuspended to 1×10^5/mL with serum-free ECM medium in a 24-well plate. The cells were observed for 24 hours. Capillary tube formation was quantified by counting the number of pixels from 3 randomly selected fields in each well under microscopy (100×).

Angiogenesis in vivo

A total of 16 six-week-old BALB/c male mice were purchased from the Shanghai Laboratory Animal Center, kept in a constant temperature specific pathogen-free (SPF) environment, and randomly divided evenly into 2 groups. All animal experiments were performed under a project license (No. 20211115c0240130) granted by committee board of Jiangnan University, in compliance with Jiangsu province guidelines for the care and use of animals. A protocol was prepared before the study without registration. A total of 4×10^6 H2170 or H1299 cells and 1×10^5 HMEC-1 cells were mixed 1:1 with Matrigel and supplemented with 30 units of heparin and 150 ng of basic fibroblast growth factor (bFGF) in a total volume of 0.5 mL and then subcutaneously injected into both flanks of mice. Two weeks later, when the tumor had grown to 1 cm^3, the mice were killed for data collection. The tumors were fixed with 4% paraformaldehyde, embedded in paraffin, sectioned, and then stained with hematoxylin and eosin. For quantitative analysis, the MVD in the tumor was counted in 3 independent fields from 3 sections (22).

Quality control, cell-type clustering, and major cell-type identification

We obtained single-ell sequencing data from lung cancer tissues according to a recent study (23). A total of 42 samples, including 22 LUSC samples, 18 LUAD samples, and 2 NSCLC samples, were examined in this study. Finally, data acquired from 90,406 cells were obtained for downstream analysis. To assign 1 of the 9 major cell types to each cluster, we scored each cluster according to the normalized expression of its canonical markers, and the highest scored cell type was assigned to each cluster. Cancer cell clusters were negative for normal lung epithelial markers and positive for epithelial cellular adhesion molecule (EpCAM). The clusters assigned to the same cell type were grouped together for the subsequent analysis. Through preliminary exploratory detection of differentially expressed genes (DEGs) in each cell cluster, combined with literature research, 9 major cell types were selected, and the DEGs were identified using the *FindMarkers* function in the "Seurat" package of R software (The Foundation for Statistical Computing).

Functional enrichment analyses

The following cutoff threshold values were used to screen for the DEGs: adjusted P value <0.01, percentage difference >10, and average log fold change (FC) >0.5. Gene set enrichment analysis (GSEA) was used to detect which gene set was significantly enriched in each specific cell cluster. Only gene sets with false-discovery rate (FDR) P values <0.05 were assessed.

Transfection

The following duplex small interfering RNAs (siRNAs) were purchased from RiboBio: si-*IRF7*-1: 5'-GAGC TGCACGTTCCTATA-3'; si-*IRF7*-2: 5'-TCGAGTGCTTCCTTATGGA-3'; si-*IFIT2*-1: 5'-GACTGGCAATAGCAAGCTA-3'; si-*IFIT2*-2: 5'-GCAACCTACTGGCCTATCT-3. 1×10^6 HMEC-1 cells were seeded in 6-well culture plates, and siRNAs were transfected into cells using Lipofectamine 2000 (Thermo America) according to the manufacturer's instructions on the next day.

Statistical analyses

GraphPad Prism 8.0 software (GraphPad Software Inc.) was used to test data with a normal distribution, and the homogeneity of variance was determined. The data are expressed as the mean ± the standard error of the mean (SEM) and were analyzed with Student *t* test (2 groups) or 1-way analysis of variance (ANOVA) with Tukey post hoc test (more than 2 groups). The data with skewed distributions were tested using nonparametric tests. The results with a P value <0.05 were considered statistically significant.

Results

LUAD tumors had a higher MVD than did LUSC tumors

Bevacizumab plays a pivotal role in the treatment of

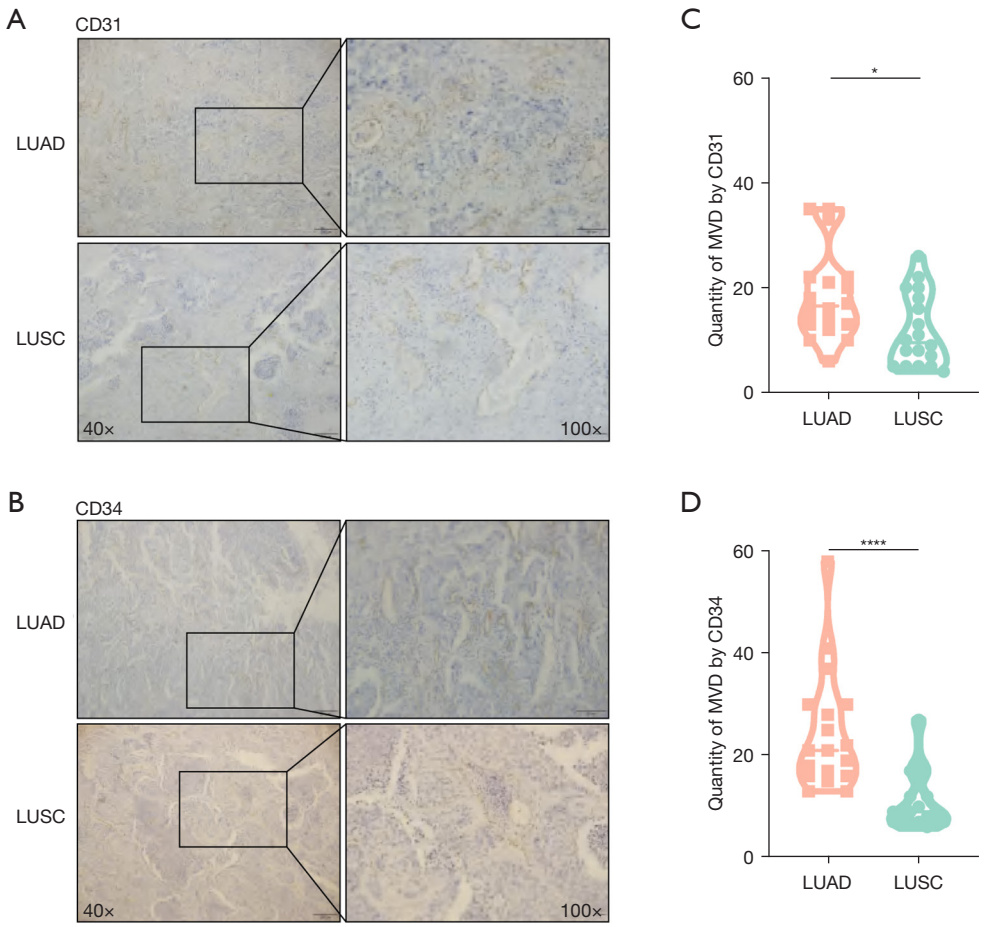

Figure 1 Microvessel density was higher in LUAD tumors than in LUSC tumors. (A) Representative electron microscopy images of microvessel densities of LUAD tumors (upper) and LUSC tumors (lower) with CD31, CD31 was stained with horseradish peroxidase (HRP). (B) Representative electron microscopy images of microvessel densities of LUAD tumors (upper) and LUSC tumors (lower) with CD34, CD34 was stained with HRP. (C) Quantification of microvessel density with CD31 staining of LUAD and LUSC tumors from image A; *P<0.05. (D) Quantification of microvessel density with CD34 staining of LUAD and LUSC tumors from image B; ****P<0.0001. LUAD, lung adenocarcinoma; LUSC, lung squamous cell carcinoma; MVD, microvessel density.

advanced lung cancer, but in patients with LUSC, it often causes substantial hemoptysis. Since bevacizumab directly targets *VEGF* to inhibit tumor angiogenesis, we compared the differences in MVD between LUAD and LUSC by staining CD31 and CD34 (*Figure 1A,1B*). We found that LUAD tumors (CD31: mean ± SEM =18.44±8.33; CD34: mean ± SEM =22.89±12.49) had a higher MVD than did LUSC tumors (CD31: mean ± SEM =11.78±6.70; CD34: mean ± SEM =10.89±5.44) (CD31: P=0.0143; CD43: P<0.0001) (*Figure 1C,1D*), suggesting that a higher MVD may contribute to less hemorrhage in certain clinical situations.

LUAD cells promoted angiogenesis more effectively than did LUSC cells

To further investigate the effect of LUAD and LUSC on angiogenic morphology, we used a tube formation assay in which capillary-like tubular structures resembling microvascular networks could be observed on Matrigel. We first assessed the effects of LUSC and LUAD cells on the capacity of HMEC-1 cells to form tubes using a coculture assay. As expected, tube formation assays showed that LUAD cells could promote endothelial cells to form more capillary tubes than could LUSC cells (LUAD: mean

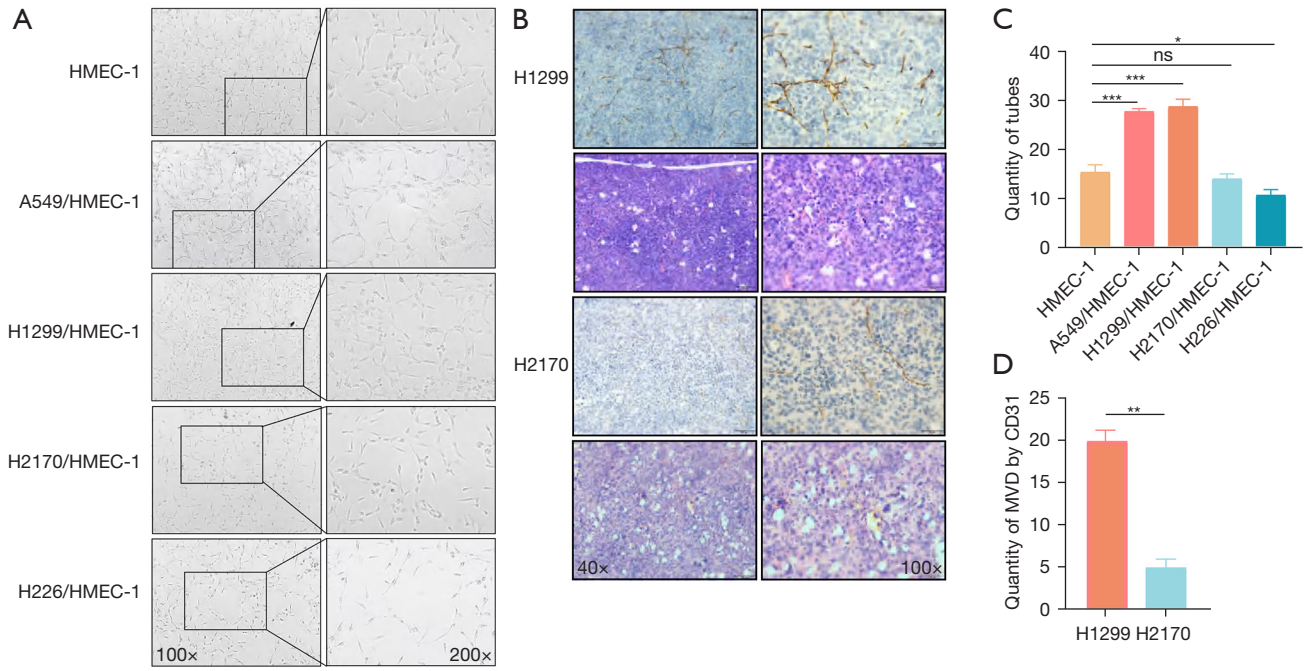

Figure 2 LUAD cells promoted angiogenesis more efficiently than did LUSC cells. (A) After 24 h three microscopic fields, selected at random, were photographed (using a 200× magnification) and the numbers of tube-like cells were counted. Representative images of HMEC-1 cells cocultured with different types of A549, H1299, H2170, H226 cells. (B) Representative electron microscopy images of microvessel densities of LUAD (upper) and LUSC (lower) cells with CD31 and HE staining. (C) Quantification of tube formation of HMEC-1 cells from image A. (D) Quantification of microvessel density with CD31 staining of LUAD and LUSC tumors from image B. *P<0.05, **P<0.01, ***P<0.001, ns, not significant. LUAD, lung adenocarcinoma; LUSC, lung squamous cell carcinoma; MVD, microvessel density; HE, hematoxylin-eosin.

± SEM =30.33±0.47; LUSC: mean ± SEM =12.33±1.25; *Figure 2*). Furthermore, we performed *in vivo* experiments by subcutaneously injecting a mixed solution containing H1299 and H2170 cells, endothelial cells, Matrigel, and various growth factors into BALB/c mice. Consistent with the *in vitro* experiments, tumors injected with LUAD cells showed a higher MVD than did those injected with LUSC cells (LUAD: mean ± SEM =19.85±0.31; LUSC: mean ± SEM =5.12±0.27 for LUSC; P<0.01; *Figure 2*).

Expression of VEGF was not significantly different between LUSC and LUAD cells

We next explored the reasons for the difference in MVD between the LUSC and LUAD tumors. *VEGF* is currently recognized as one of the most relevant targets for angiogenesis, and bevacizumab is an antagonist of *VEGF*. We analyzed whether the difference in MVD was caused by the different levels of *VEGF* secreted from tumor cells after acting on endothelial cells. Thus, we first detected the expression of *VEGF* in A549, H1299, H358, H2170, H226 and H1703 cells using Western blotting (*Figure 3A*), qRT-PCR (*Figure 3B*), ELISA (*Figure 3C*), and immunofluorescence (*Figure 3D*). We found that there was no significant difference in the expression of *VEGF* between LUSC and LUAD cells. These results suggested that *VEGF* expression in NSCLC tumor cells has no effect on the difference in angiogenesis.

Bioinformatic analysis indicated the heterogeneity of gene expression between LUAD and LUSC

We next investigated the DEGs in endothelial cells from LUAD and LUSC tumors. Lung cancer single-cell sequencing data were obtained from a recent study (23). The 42 samples in this study included 22 LUAD, 18 LUSC and 2 NSCLC samples with accurately defined pathological types. After the final quality control, we obtained data

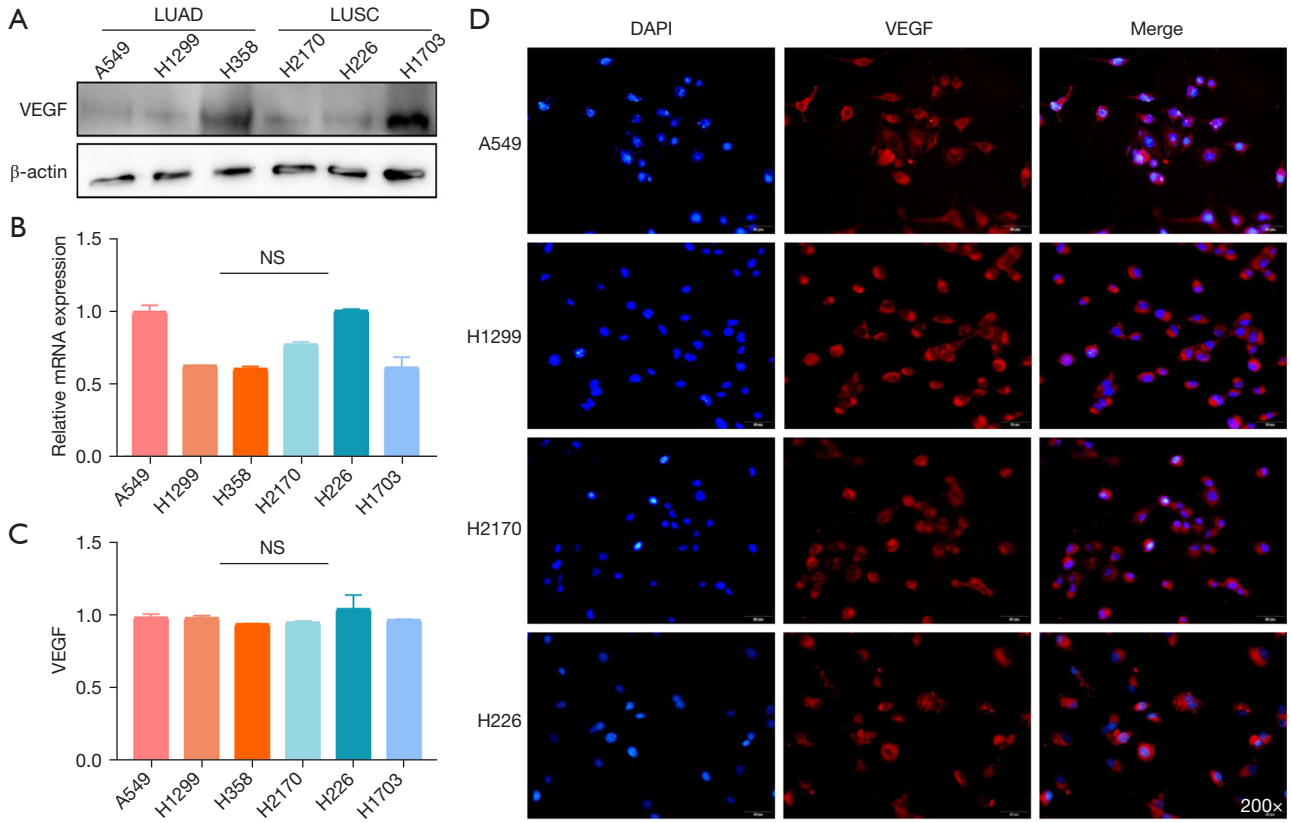

Figure 3 The expression of *VEGF* was not significantly different between LUSC and LUAD cells. (A) The protein levels of *VEGF* were determined with Western blot assays in NSCLC cell lines, with β-actin protein serving as an internal control. (B) Relative mRNA expression of *VEGF* in NSCLC cells. (C) The expression of *VEGF* in NSCLC cells supernatant according to ELISA. (D) The expression of *VEGF* in NSCLC cells was detected using immunofluorescence. NS, not significant. *VEGF*, vascular endothelial growth factor; NSCLC, non-small cell lung cancer; LUAD, lung adenocarcinoma; LUSC, lung squamous cell carcinoma; ELISA, enzyme linked immunosorbent assay; DAPI, 4,6-diamino-2-phenylindole.

regarding 24,666 LUAD cells, 57,774 LUSC cells. And 7447 other types (*Figure 4A*). We clustered these cells into 9 groups according to their marker genes, including clusters of immune cells, stromal cells, and epithelial cells (*Figure 4B*,*4C*). The results showed that there was a high degree of heterogeneity between LUAD and LUSC in the composition of cells in the tumor microenvironment, especially malignant epithelial cells and endothelial cells. Next, we identified the DEGs in malignant epithelial cells and endothelial cells in LUAD and LUSC tumors. Furthermore, the GSEA results based on the 3 data sets suggested that many signaling pathways related to angiogenesis were significantly enriched (*Figure 4D*,*4E*), including the interferon-α response, KRAS signaling up, and P53 signaling pathways. Finally, we analyzed the signaling pathway between LUSC and LUAD through the DEGs (*Figure 4F*,*4G*), the data showed that there were significant differences in signaling pathways between the two groups.

IRF7 and IFIT2 were differentially expressed in LUSC and LUAD cells

We subsequently searched for the DEGs involved in these pathways according to the frequency of occurrence in each pathway, and in combination with a review of the literature, the results indicated the angiogenesis-related genes for subsequent analyses. The selected genes are shown in *Figure 5A*. To further verify these candidate genes in tumor endothelial cells, we cocultured LUAD and LUSC cell lines with HMEC-1 cells and verified that interferon regulatory factor 7 (*IRF7*) was upregulated in endothelial cells

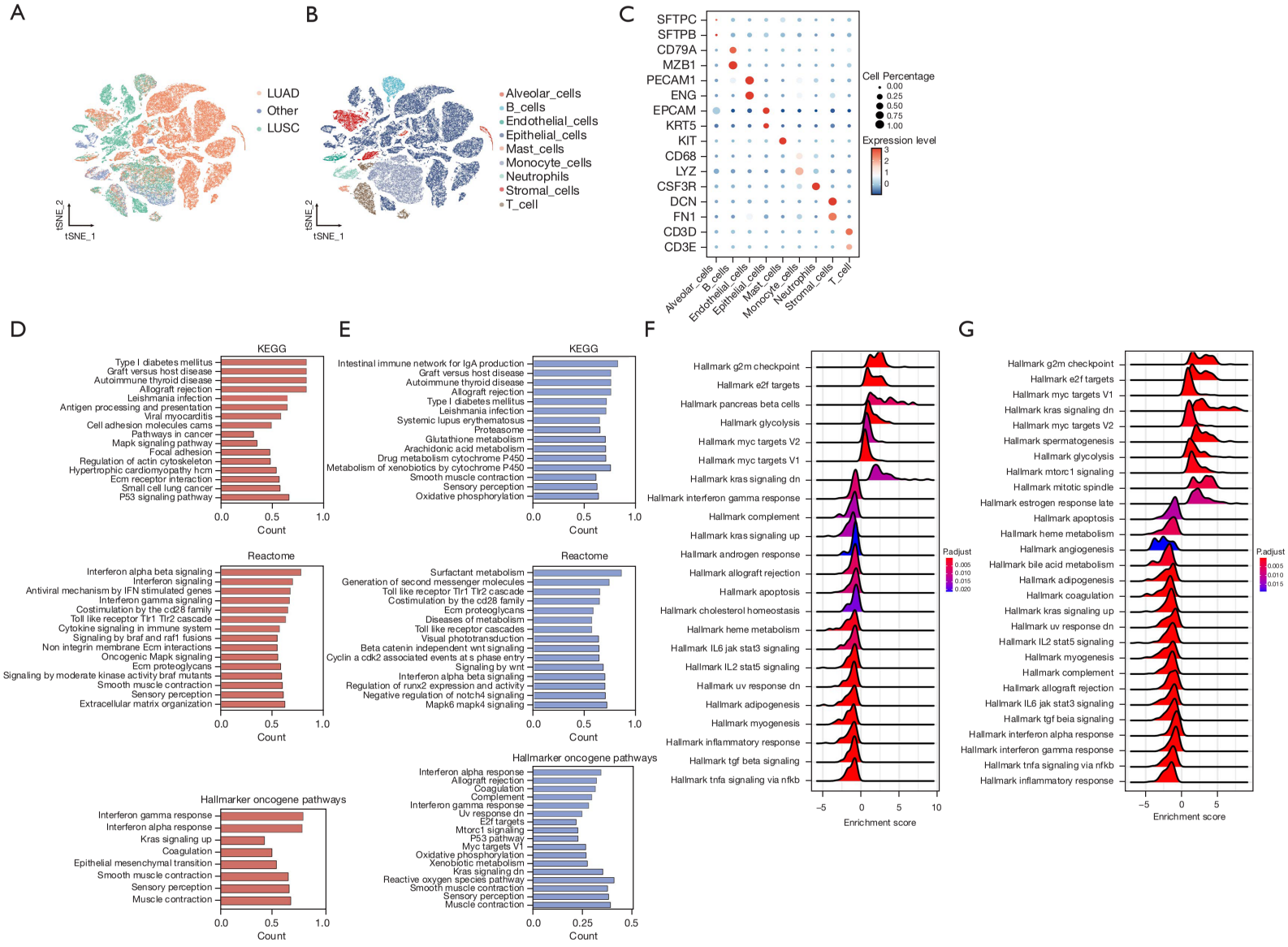

Figure 4 Bioinformatic analysis indicated the heterogeneity of gene expression between LUAD and LUSC. (A) The t-SNE plot showing cell origins. (B) The t-SNE plot showing the annotation and color codes for cell types in the NSCLC ecosystem. (C) Heatmap showing the expression of marker genes in the indicated cell types. (D,E) Bar chart showing the enrichment of specific pathways based on the hallmark gene set/KEGG/a of different genes between endothelial (left) and epithelial (right) cells. (F,G) The difference in signal pathways between LUAD (left) and LUSC (right). NSCLC, non-small cell lung cancer; LUAD, lung adenocarcinoma; LUSC, lung squamous cell carcinoma; t-SNE, t-distributed stochastic neighbor embedding; KEGG, Kyoto Encyclopedia of Genes and Genomes

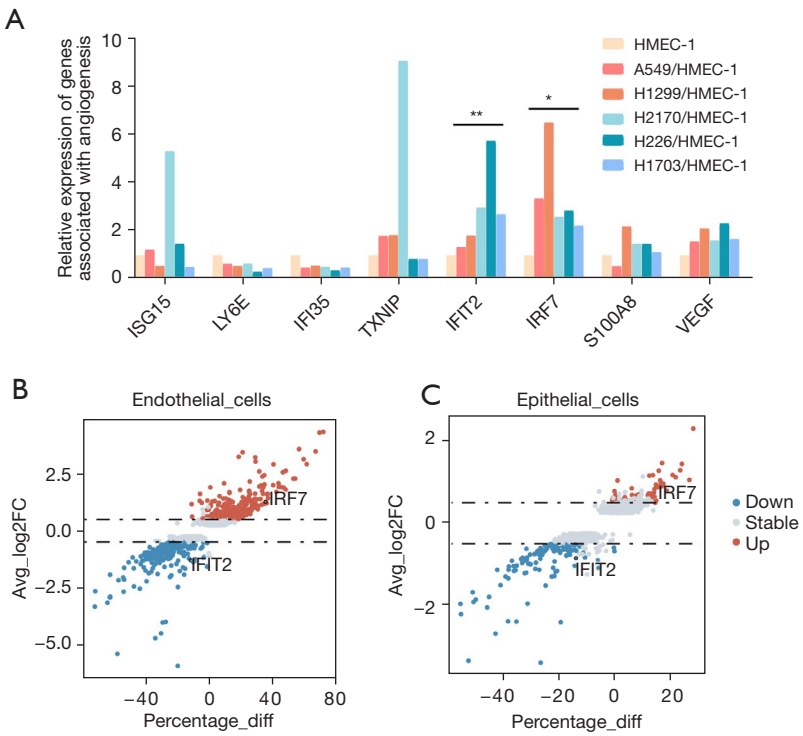

Figure 5 *IRF7* and *IFIT2* were differentially expressed in LUSC and LUAD cells. (A) Relative expression of genes associated with angiogenesis in HMEC-1 cells cocultured with A549, H1299, H2170, H226, H1703 cells at 37 ℃ for 72 h. (B,C) Volcano plot showing the differentially expressed genes between LUAD and LUSC tumors in endothelial or epithelial cells. *P<0.05, **P<0.01. *ISG15*, interferon stimulated gene 15; *LY6E*, lymphocyte antigen 6; *IFI35*, interferon-induced protein 35; *TXNIP*, thioredoxin interacting protein; *IFIT2*, interferon-induced protein with tetratricopeptide repeats 2; *IRF7*, interferon regulatory factor 7; *S100A8*, S100 calcium binding protein A8; LUAD, lung adenocarcinoma; LUSC, lung squamous cell carcinoma; FC, fold change.

cocultured with LUAD cells and that interferoninduced protein with tetratricopeptide repeats 2 (*IFIT2*) was upregulated in endothelial cells cocultured with LUSC cells (*Figure 5A*). A volcano plot also showed that among these candidate genes, *IFIT2* and *IRF7* were enriched in the epithelial cells of NSCLC tumors. These results suggested that the 2 genes may play an important role in angiogenesis (*Figure 5B,5C*). Therefore, we focused on these 2 genes in the subsequent investigations.

IRF7 and IFIT2 regulated the tube formation of HMEC-1 cells

IRF7 is the most important nuclear transcription factors regulating type-I interferon (IFN) production in mammals (24). *IFIT2* is an interferon-stimulated gene with well-established antiviral activity but limited mechanistic understanding (25). In order to determine whether the microvascular differences between LUAD and LUSC were caused by *IRF7* and *IFIT2*, we used 2 small interference sequences to knockdown *IRF7* and *IFIT2* (*Figure 6A,6B*). Then, HMEC-1 cells transfected with these small interferences were spread on Matrigel for ring formation evaluation (*Figure 6C*). We found that *IRF7* knockdown significantly inhibited the ring formation of HMEC-1 cells, whereas *IFIT2* knockdown promoted the ring formation of HMEC-1 cells. Taken together, these data suggest that the difference in the expression of *IRF7* and *IFIT2* in the microvasculature leads to the difference in MVD between the LUSC and LUAD tumors.

Bevacizumab promoted the effects of IRF7 and IFIT2 on angiogenesis

To explore whether bevacizumab regulates the expression of *IRF7* and *IFIT2* in endothelial cells as well as the angiogenesis of lung cancer cells, bevacizumab was added to HMEC-1 cells cocultured with H1299 and H2170 cells.

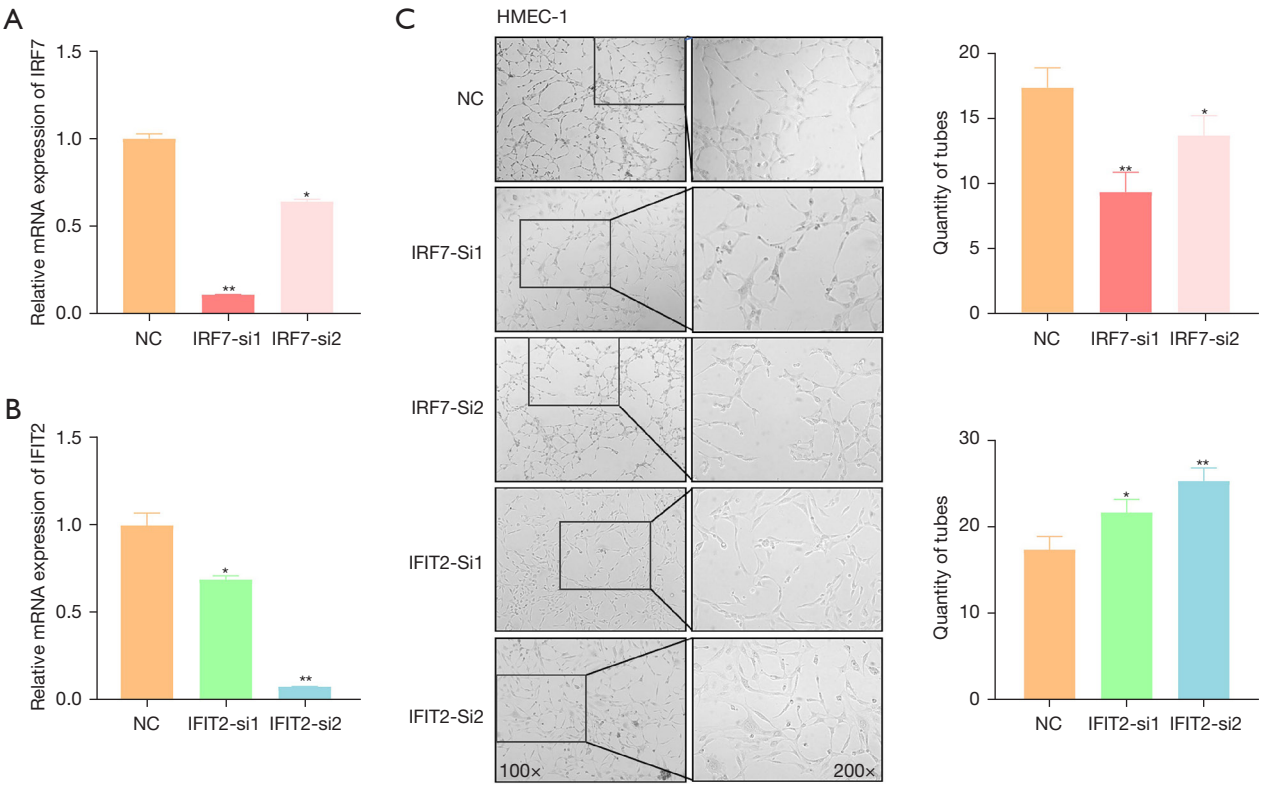

Figure 6 *IRF7* and *IFIT2* regulate the tube formation of HMEC-1 cells. (A,B) The knockdown efficacy of *IRF7* and *IFIT2* in HMEC-1 cells was determined using qRT-PCR. (C) Three microscopic fields, selected at random, were photographed (using a 200× magnification) and the numbers of tube-like cells were counted. Representative images of HMEC-1 cells on Matrigel that were subjected to *IRF7* and *IFIT2* knockdown with siRNA. HMEC-1 cells were added to 24-well plates and incubated at 37 ℃ for 24 h. The tube formation of HMEC-1 cells was observed. *P<0.05, **P<0.01. *IRF7*, interferon regulatory factor 7; *IFIT2*, interferoninduced protein with tetratricopeptide repeats 2; qRT-PCR, real time quantitative PCR; siRNA, small interfering RNA; NC, normal control.

As shown in *Figure 7A*, after bevacizumab treatment (26), HMEC-1 cells cocultured with H1299 cells formed more rings than did those cocultured with H2170 cells (H1299 cell culture mean ± SEM =22.33±1.25; H2170 culture: mean ± SEM =9.67±1.70; P=0.03). Although the expression of *VEGF* and *VEGFA* in HMEC-1 cells was downregulated, there were no statistically significant differences between the 2 groups (*Figure 7B*,*7C*). Interestingly, after the addition of bevacizumab, *IRF7* and *IFIT2* levels in HMEC-1 cells cocultured with H1299 and H2170 cells changed even more strikingly than did those in the noncoculture group (*Figure 7D*,*7E*). We speculate that bevacizumab could further enhance the effect of these 2 genes on angiogenesis.

Discussion

In recent years, the prevalence of lung cancer has increased rapidly in China (1,27), and traditional radiotherapy and chemotherapy have been unable to meet treatment expectations. The emergence of bevacizumab has provided a new treatment strategy for lung cancer. Several studies (28,29) have shown that bevacizumab-based therapy may lead to longer survival and significantly prolonged disease remission in patients with advanced NSCLC. However, patients with LUSC are prone to massive hemoptysis during bevacizumab treatment. Due to this serious side effect, bevacizumab has limited use in patients with LUSC. In this study, we explored the causes underlying the differences in hemoptysis in patients with LUSC and LUAD after bevacizumab treatment.

First, we found that LUSC tumors showed lower angiogenesis than LUAD tumors, which was further confirmed by *in vitro* and *in vivo* experiments. *VEGF* is a key regulator of angiogenesis. Therefore, we aimed to explore

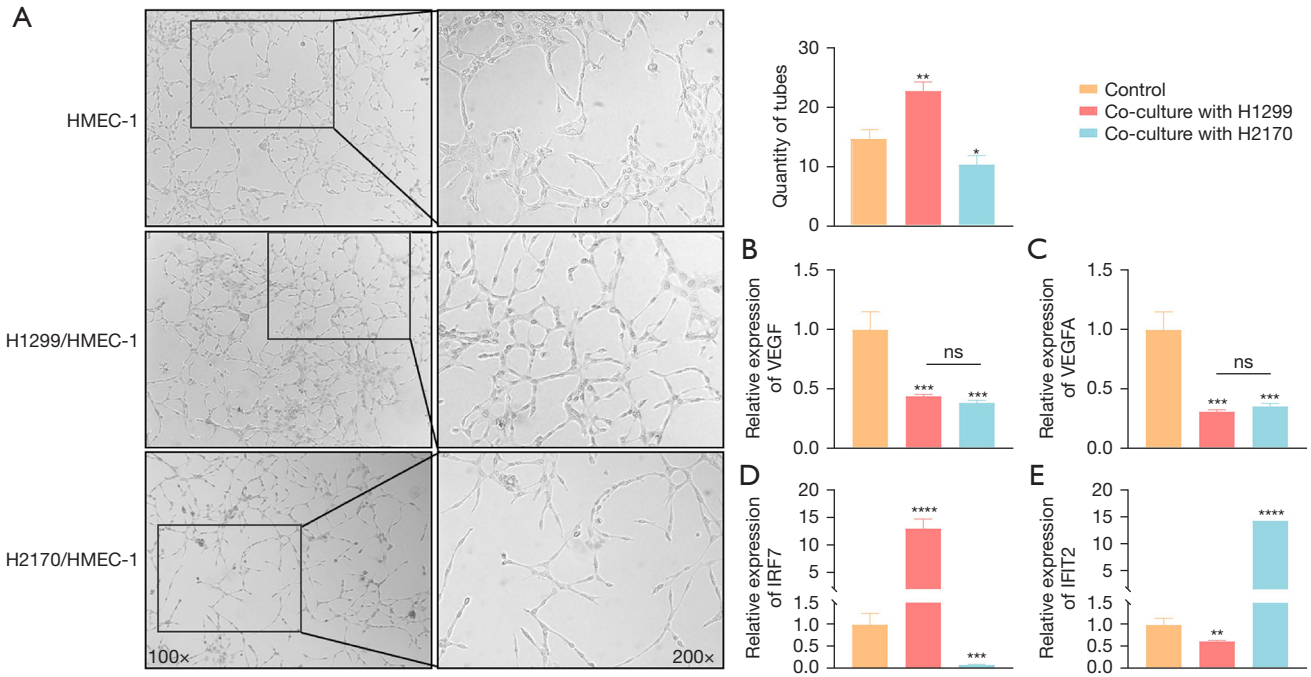

Figure 7 Bevacizumab promoted the effects of *IRF7* and *IFIT2* on angiogenesis. (A) After 24 h three microscopic fields, selected at random, were photographed (using a 200× magnification) and the numbers of tube-like cells were counted. Representative images of HMEC-1 cells on Matrigel that were treated with bevacizumab and cocultured with different types of H1299 and H2170 cells. (B-E) Relative expression of *VEGF*, *VEGFA*, *IRF7*, and *IFIT2* in HMEC-1 cells treated with bevacizumab and cocultured with H1299 cells and H2170 cells. *P<0.05, **P<0.01, ***P<0.001, ****P<0.0001, ns, not significant. *IRF7*, interferon regulatory factor 7; *IFIT2*, interferoninduced protein with tetratricopeptide repeats 2; *VEGF*, vascular endothelial growth factor; *VEGFA*, vascular endothelial growth factor A.

the differences in *VEGF* expression between LUSC and LUAD tumors, but no significant difference was observed.

We then downloaded single-cell sequencing data obtained from patients with NSCLC and investigated the pathways and genes related to angiogenesis. The results, combined with the experimental verification, indicated that *IRF7* was highly expressed in the endothelial cells of LUAD tumors and that *IFIT2* was highly expressed in the endothelial cells of LUSC tumors. Simons *et al.* reported that IRF3 and *IRF7* mediate neoangiogenesis through inflammatory cytokines (30). Lai *et al.* showed that *IFIT2* depletion promotes angiogenesis in metastatic oral squamous cell carcinoma cells (31). These results, all of which are consistent with the observations of study, suggest that *IRF7* promotes angiogenesis and that *IFIT2* inhibits angiogenesis. Our functional evaluations also showed that *IRF7* knockdown reduced the number of vascular loops and decreased lumen integrity, whereas knockdown of *IFIT2* increased the number of vascular loops and improved lumen integrity. Moreover, bevacizumab treatment further promoted the effects of *IRF7* and *IFIIT2* on angiogenesis in lung cancer. Taken together, these results suggest that the difference in the expression of *IRF7* and *IFIT2* may affect the angiogenesis of LUSC and LUAD tumors.

Investigations of patients with LUSC who are prone to massive hemoptysis after treatment with bevacizumab have mainly focused on macroscopic aspects such as anatomy. In this study, for the first time, we explored the DRGs in tumor endothelial cells in patients with LUSC and LUAD using single-cell sequencing analysis. A differential expression of *IRF7* and *IFIT2* was observed in LUSC and LUAD cells and was associated with low MVD in LUSC tissue and less blood supply inside the tumor. It is generally believed that MVD is positively correlated with the risk of bleeding. Dansin *et al.* collected the clinical data of 222 patients with NSCLC treated with bevacizumab to explore potential associations between bleeding events and baseline and disease characteristics. It was found that the overall bleeding rate of noncentral tumors was higher than that of central lung cancer, whereas the incidence of

bleeding grade ≥3 was lower (32). According to the 2004 World Health Organization (WHO) classification, LUSC is mainly a central-type lung cancer that occurs in the trachea and bronchus, and approximately 65% of LUAD cases are the peripheral type (33). Synthesizing these finding's with our results, we hypothesized that due to the differential expression of *IRF7* and *IFIT2*, LUAD has a higher MVD and overall bleeding risk. In addition, due to the abundant blood supply, there is a lower risk of intratumoral cavitation and fatal hemorrhage.

Moreover, some researchers believe that tumors with sufficient MVD do not exhibit activation of hypoxia-induced signaling pathways; therefore, they remain sensitive to chemotherapy and radiotherapy, and the lack of such signaling may lead to reduced tumor invasiveness. Similarly, low MVD is associated with higher tumor aggressiveness, which causes a greater degree of vascular infiltration and leads to bleeding. Our study suggests that the difference in the expression of *IRF7* and *IFIT2* in the endothelium of LUSC and LUAD tumors causes the difference in MVD between these 2 tumor types. After bevacizumab treatment, the effect of *IRF7* and *IFIT2* on angiogenesis is further amplified, reducing tumor angiogenesis in LUSC, decreasing vascular stability, increasing tissue hypoxia, and increasing the incidence of hemoptysis.

In this study, we identified the differential expression of *IRF7* and *IFIT2* in the endothelium of LUSC and LUAD tumors and showed that bevacizumab may affect angiogenesis by enhancing the effect of *IRF7* and *IFIT2*. However, the molecular mechanisms by which *IRF7* and *IFIT2* participate in and regulate angiogenesis-related pathways and mediate angiogenesis after bevacizumab treatment remain unclear. Our findings clarify the important roles of *IRF7* and *IFIT2* in angiogenesis-related pathways. Thus, we can prevent the substantial hemoptysis caused by bevacizumab treatment by targeting the levels of *IRF7* and *IFIT2* in patients with LUSC. Overall, this study can help improve clinical treatment strategies for these patients.

Conclusions

The MVD of LUAD tissues was higher than that of LUSC tissues. Higher *IRF7* levels and lower *IFIT2* levels in LUAD tumors were associated with a higher MVD in LUAD tissues, which may be responsible for the different hemorrhage outcomes after bevacizumab treatment.

Acknowledgments

Funding: This work was supported by National Natural Science Foundation of China (No. 82173193); the Natural Science Foundation of Jiangsu Province (No. BK20211033); Science and Technology Demonstration Project of Social Development of Jiangsu Province (No. BE2019631); the Double Hundred Medical Professionals Program of Wuxi (Nos. BJ2020053 and BJ2020058); the Wuxi Taihu Lake Talent Plan, Wuxi Medical Key Discipline (No. ZDXK2021002); and the Project of State Key Laboratory of Radiation Medicine and Protection, Soochow University (No. GZK1202202).

Footnote

Reporting Checklist: The authors have completed the MDAR and ARRIVE reporting checklists. Available at https://jtd.amegroups.com/article/view/10.21037/jtd-23-389/rc

Data Sharing Statement: Available at https://jtd.amegroups.com/article/view/10.21037/jtd-23-389/dss

Peer Review File: Available at https://jtd.amegroups.com/article/view/10.21037/jtd-23-389/prf

Conflicts of Interest: All authors have completed the ICMJE uniform disclosure form (available at https://jtd.amegroups.com/article/view/10.21037/jtd-23-389/coif). The authors have no conflicts of interest to declare.

Ethical Statement: The authors are accountable for all aspects of the work in ensuring that questions related to the accuracy or integrity of any part of the work are appropriately investigated and resolved. The study was approved by the Clinical Research Ethics Committees of Affiliated Hospital of Jiangnan University (No. LS2021019), and written informed consent was obtained from all patients. The study was conducted in accordance with the Declaration of Helsinki (as revised in 2013). All animal experiments were performed under a project license (No. 20211115c0240130) granted by committee board of Jiangnan University, in compliance with Jiangsu province guidelines for the care and use of animals. A protocol was prepared before the study without registration.

References

1. Sung H, Ferlay J, Siegel RL, et al. Global Cancer Statistics 2020: GLOBOCAN Estimates of Incidence and Mortality Worldwide for 36 Cancers in 185 Countries. CA Cancer J Clin 2021;71:209-49.
2. Thai AA, Solomon BJ, Sequist LV, et al. Lung cancer. Lancet 2021;398:535-54.
3. Bogos K, Kiss Z, Tamási L, et al. Improvement in lung cancer survival: Six-year survival analysis of patients diagnosed between 2011 and 2016 in Hungary. J Clin Oncol 2020;38:e21582.
4. Johnson DH, Fehrenbacher L, Novotny WF, et al. Randomized phase II trial comparing bevacizumab plus carboplatin and paclitaxel with carboplatin and paclitaxel alone in previously untreated locally advanced or metastatic non-small-cell lung cancer. J Clin Oncol 2004;22:2184-91.
5. Tan AC, Tan DSW. Targeted Therapies for Lung Cancer Patients With Oncogenic Driver Molecular Alterations. J Clin Oncol 2022;40:611-25.
6. Mayekar MK, Bivona TG. Current Landscape of Targeted Therapy in Lung Cancer. Clin Pharmacol Ther 2017;102:757-64.
7. Hou X, Zhou C, Wu G, et al. Efficacy, Safety, and Health-Related Quality of Life With Camrelizumab Plus Pemetrexed and Carboplatin as First-Line Treatment for Advanced Nonsquamous NSCLC With Brain Metastases (CAP-BRAIN): A Multicenter, Open-Label, Single-Arm, Phase 2 Study. J Thorac Oncol 2023. [Epub ahead of print]. doi: 10.1016/j.jtho.2023.01.083.
8. Yu Y, Yang Y, Li H, et al. Targeting HER2 alterations in non-small cell lung cancer: Therapeutic breakthrough and challenges. Cancer Treat Rev 2023;114:102520.
9. Breen WG, Leventakos K, Dong H, et al. Radiation and immunotherapy: emerging mechanisms of synergy. J Thorac Dis 2020;12:7011-23.
10. Zhao Z, Zhao L, Xia G, et al. Efficacy and safety of bevacizumab biosimilar compared with reference bevacizumab in locally advanced and advanced non-small cell lung cancer patients: A retrospective study. Front Oncol 2022;12:1036906.
11. Long J, Lei S, Wu Z, et al. Efficacy and safety of original EGFR-TKI combined with bevacizumab in advanced lung adenocarcinoma patients harboring EGFR-mutation experiencing gradual progression after EGFR-TKI treatment: a single-arm study. Ann Transl Med 2022;10:1334.
12. Margolin K, Gordon MS, Holmgren E, et al. Phase Ib trial of intravenous recombinant humanized monoclonal antibody to vascular endothelial growth factor in combination with chemotherapy in patients with advanced cancer: pharmacologic and long-term safety data. J Clin Oncol 2001;19:851-6.
13. Sandler A, Gray R, Perry MC, et al. Paclitaxel-carboplatin alone or with bevacizumab for non-small-cell lung cancer. N Engl J Med 2006;355:2542-50.
14. Jin F, Li Q, Bai C, et al. Chinese Expert Recommendation for Diagnosis and Treatment of Massive Hemoptysis. Respiration 2020;99:83-92.
15. Hellmann MD, Chaft JE, Rusch V, et al. Risk of hemoptysis in patients with resected squamous cell and other high-risk lung cancers treated with adjuvant bevacizumab. Cancer Chemother Pharmacol 2013;72:453-61.
16. Reck M, Barlesi F, Crinò L, et al. Predicting and managing the risk of pulmonary haemorrhage in patients with NSCLC treated with bevacizumab: a consensus report from a panel of experts. Ann Oncol 2012;23:1111-20.
17. Salajka F. Occurrence of haemoptysis in patients with newly diagnosed lung malignancy. Schweiz Med Wochenschr 1999;129:1487-91.
18. Goto K, Endo M, Kusumoto M, et al. Bevacizumab for non-small-cell lung cancer: A nested case control study of risk factors for hemoptysis. Cancer Sci 2016;107:1837-42.
19. Iordache S, Saftoiu A, Georgescu CV, et al. Vascular endothelial growth factor expression and microvessel density--two useful tools for the assessment of prognosis and survival in gastric cancer patients. J Gastrointestin Liver Dis 2010;19:135-9.
20. Pomme G, Augustin F, Fiegl M, et al. Detailed assessment of microvasculature markers in non-small cell lung cancer reveals potentially clinically relevant characteristics. Virchows Arch 2015;467:55-66.
21. Hu P, Wang G, Cao H, et al. Haemoptysis as a prognostic factor in lung adenocarcinoma after curative resection. Br J Cancer 2013;109:1609-17.
22. Li J, Zhang Y, Liu Y, et al. Microvesicle-mediated transfer

of microRNA-150 from monocytes to endothelial cells promotes angiogenesis. J Biol Chem 2013;288:23586-96.
23. Wu F, Fan J, He Y, et al. Single-cell profiling of tumor heterogeneity and the microenvironment in advanced non-small cell lung cancer. Nat Commun 2021;12:2540.
24. Lin Z, Wang J, Zhao S, et al. Goose IRF7 is involved in antivirus innate immunity by mediating IFN activation. Dev Comp Immunol 2022;133:104435.
25. Tran V, Ledwith MP, Thamamongood T, et al. Influenza virus repurposes the antiviral protein IFIT2 to promote translation of viral mRNAs. Nat Microbiol 2020;5:1490-503.
26. Schicher N, Paulitschke V, Swoboda A, et al. Erlotinib and bevacizumab have synergistic activity against melanoma. Clin Cancer Res 2009;15:3495-502.
27. Bray F, Ferlay J, Soerjomataram I, et al. Global cancer statistics 2018: GLOBOCAN estimates of incidence and mortality worldwide for 36 cancers in 185 countries. CA Cancer J Clin 2018;68:394-424.
28. Zhou Y, He M, Li R, et al. The Safety and Effectiveness of Bevacizumab in the Treatment of Nonsquamous Non-Small-Cell Lung Cancer: A Meta-Analysis of Randomized Controlled Trials. Biomed Res Int 2021;2021:5537899.
29. Semrad TJ, Redman MW, Herbst RS, et al. Outcomes for patients treated with or without bevacizumab on SWOG S0819: A randomized, phase III study comparing carboplatin/Paclitaxel or carboplatin/Paclitaxel/bevacizumab with or without concurrent cetuximab in patients with advanced non-small cell lung cancer (NSCLC). J Clin Oncol 2016;34:9082.
30. Simons KH, de Vries MR, de Jong RCM, et al. IRF3 and IRF7 mediate neovascularization via inflammatory cytokines. J Cell Mol Med 2019;23:3888-96.
31. Lai KC, Liu CJ, Lin TJ, et al. Blocking TNF-α inhibits angiogenesis and growth of IFIT2-depleted metastatic oral squamous cell carcinoma cells. Cancer Lett 2016;370:207-15.
32. Dansin E, Cinieri S, Garrido P, et al. MO19390 (SAiL): bleeding events in a phase IV study of first-line bevacizumab with chemotherapy in patients with advanced non-squamous NSCLC. Lung Cancer 2012;76:373-9.
33. Petersen I, Warth A. Lung cancer: developments, concepts, and specific aspects of the new WHO classification. J Cancer Res Clin Oncol 2016;142:895-904.

(English Language Editor: J. Gray)

Cite this article as: Huang L, Yin Y, Qian D, Cao Y, Wang D, Wu X, Ming L, Huang Z, Zhou L. *IRF7* and *IFIT2* in mediating different hemorrhage outcomes for non-small cell lung cancer after bevacizumab treatment. J Thorac Dis 2023;15(4):2022-2036. doi: 10.21037/jtd-23-389